DISCLAIMER

This report was prepared as an account of work sponsored by an agency of the United States Government. Neither the United States Government nor any agency thereof, nor any of their employees, makes any warranty, express or implied, or assumes any legal liability or responsibility for the accuracy, completeness, or usefulness of any information, apparatus, product, or process disclosed, or represents that its use would not infringe privately owned rights. Reference herein to any specific commercial product, process, or service by trade name, trademark, manufacturer, or otherwise does not necessarily constitute or imply its endorsement, recommendation, or favoring by the United States Government or any agency thereof. The views and opinions of authors expressed herein do not necessarily state or reflect those of the United States Government or any agency thereof. Reference herein to any social initiative (including but not limited to Diversity, Equity, and Inclusion (DEI); Community Benefits Plans (CBP); Justice 40; etc.) is made by the Author independent of any current requirement by the United States Government and does not constitute or imply endorsement, recommendation, or support by the United States Government or any agency thereof.

U.S. DEPARTMENT OF ENERGY | Office of Science

DOE/SC-ARM-TR-326

Infrared Cloud Imager Instrument Intercomparison Report

N Pust
A Beard
C McCann
P Nugent

November 2025

ARM

DISCLAIMER

DOE/SC-ARM-TR-326

Infrared Cloud Imager Instrument Intercomparison Report

N Pust
C McCann
A Beard
P Nugent
All at NWB Sensors

November 2025

How to cite this document:

Pust, N, C McCann, A Beard, and P Nugent. Infrared Cloud Imager Instrument Intercomparison Report. U.S. Department of Energy, Atmospheric Radiation Measurement User Facility, Richland, Washington. DOE/SC-ARM-TR-326.

Work supported by the U.S. Department of Energy,
Office of Science, Office of Biological and Environmental Research

Acronyms and Abbreviations

AERI	atmospheric emitted radiance interferometer
ARM	Atmospheric Radiation Measurement
FPC	fixed-pattern correction
GNSS	Global Navigational Satellite System
ICI	infrared cloud imager
MODTRAN	MODerate resolution atmospheric TRANsmission
NetCDF	Network Common Data Form
PWV	precipitable water vapor
SGP	Southern Great Plains
UTC	Coordinated Universal Time

Contents

Figures

1.0 Summary

The Infrared Cloud Imager Instrument Intercomparison was a guest instrument deployment by NWB Sensors to the U.S. Department of Energy's Atmospheric Radiation Measurement (ARM) User Facility observatory on the Southern Great Plains (SGP) between May 18 and December 12, 2023. NWB Sensors is a company that has developed a commercially available infrared cloud imager (ICI). The ICI provides radiometrically calibrated, full-sky images of the downwelling infrared radiance in the 7.3-14 µm band. In addition, it provides cloud radiance as the residual between the observed radiance and the modeled cloud-free radiance as well as derived cloud products. The instrument is used in applications that require consistent detection of clouds across day and night. For more information, consult the instrument's webpage.

Figure 1. Infrared cloud imager with its integrated weather sensor deployed on SGP's guest instrument platform.

The primary goal of the deployment was to validate the radiometric accuracy of the ICI. The ICI uses a proprietary calibration method to convert the raw data from its infrared camera into downwelling radiance. Unlike similar instruments, the system does not have an onboard blackbody calibration standard. Instead, NWB Sensors characterizes each ICI camera individually in an environmental chamber while looking at a blackbody standard. The resulting (proprietary) calibration is used operationally in the instrument and has been demonstrated to be stable over long periods. To validate the radiometric products from the ICI, an intercomparison between the ICI data products and those from ARM's atmospheric emitted radiance interferometer (AERI) was made. The AERI is a best-in-class instrument for measuring downwelling infrared radiance (Gero et al. 2025). A weighted integration of the AERI's spectral radiances across the ICI's camera response was performed. The resulting radiance (herein called the AERI radiance) was directly compared to the zenith radiance concurrently observed by the ICI. The results of these comparisons are reported in the next section of this report.

The SGP deployment was also used to validate other portions of the ICI processing. A proprietary model within the ICI is used to simulate a cloud-free sky. This model uses surface meteorology and precipitable water vapor (PWV) to predict the downwelling radiance from a cloud-free sky for the ICI camera's response. This simulated radiance is subtracted from the observed radiance to determine the residual

radiance associated with clouds. This residual radiance is then used to derive cloud data products. Consequently, the accuracy of these cloud-free models can limit the ability of the ICI to detect thin clouds. As with the ICI's observed radiance, the radiance values predicted from the cloud-free model were compared to the AERI radiances observed. The results are reported below.

Finally, the PWV products from the ICI were validated. The ICI uses an onboard PWV retrieval system that is independent of the imager. This system uses raw GNSS (Global Navigational Satellite System) observations with corresponding precise clock and orbit corrections to observe PWV in real time. (The method implemented generally follows the method described in Bevis 1992.) The observed PWV values are used in the cloud-free radiance model that was previously described. For the SGP deployment, the PWV observations from the GNSS-based system were compared to those from ARM's microwave radiometer and those calculated from balloon-borne sounding system (radiosonde) observations. The results are reported below.

Since the instrument was still in development during this 2023 SGP campaign and several software bugs were not resolved, intermittent outages occurred routinely whenever the instrument tried to recover itself. In addition, several extended outages occurred on Jun 24-25, Jul 26-Aug 1, Sept 11-12, Oct 24-25, Oct 28-29, Nov 24-27, and Dec 4-5. Also, ICI data products are susceptible to dirt or debris on the lens. These contaminants manifest as isolated spots and/or thin clouds in the imagery that cannot easily be removed in post-processing. During deployment, ARM staff would clean the lens when advised, but there are periods where significant levels of dust, pollen, and water spots accumulated before being noticed. Rain drops and one instance of what appears to be bird droppings can be seen in the data from Jul 7 14:38 to Jul 10 14:07. There is water on the lens from 6:00 to 12:30 on Jul 18. Balloon-borne soundings are visible on select days. (All times given are UTC.)

In addition, the data from the SGP AERI were compromised from April to 2 Aug 2023. While making our initial comparisons, we found that something was very wrong with the reported AERI spectral radiances and contacted the instrument mentor. After investigation, ARM staff found bird droppings on the AERI scan mirror that caused an offset in the spectral radiances. In addition, the ICI lens was cleaned on Aug 28, which caused more than a 1-W/m^{2}Sr shift in the data. Therefore, only data taken after Aug 28 are used in this study.

The ICI data collected during this campaign have been uploaded to the ARM Data Center. Each raw image and its associated data products are stored in a single NetCDF file. These were collected at a 1-minute interval. In addition, a video time lapse that renders the most important ICI data products is included with data as a courtesy to the user. We advise downloading and viewing this video prior to using the ICI data products.

2.0 Results

The most beneficial result of this instrument intercomparison was a major modification to our calibration method. Preliminary comparisons of the integrated radiance derived from the AERI and the ICI radiance showed small but significant differences that varied approximately on a diurnal period. This "anomalous radiance" was determined to be linearly correlated with surface temperature and lens temperature (see Figure 2). This result prompted a year-long investigation into the ICI's calibration methodology. We determined that several of our calibration coefficients were overdetermined. After considering both the

SGP ICI data and data collected from other deployments, we developed a new calibration method that resolves these issues. Then, the ICI data from this SGP campaign were reprocessed using this new calibration method. The recalibrated ICI data was submitted to the ARM Data Center and were used to create the comparisons below (except Figure 2).

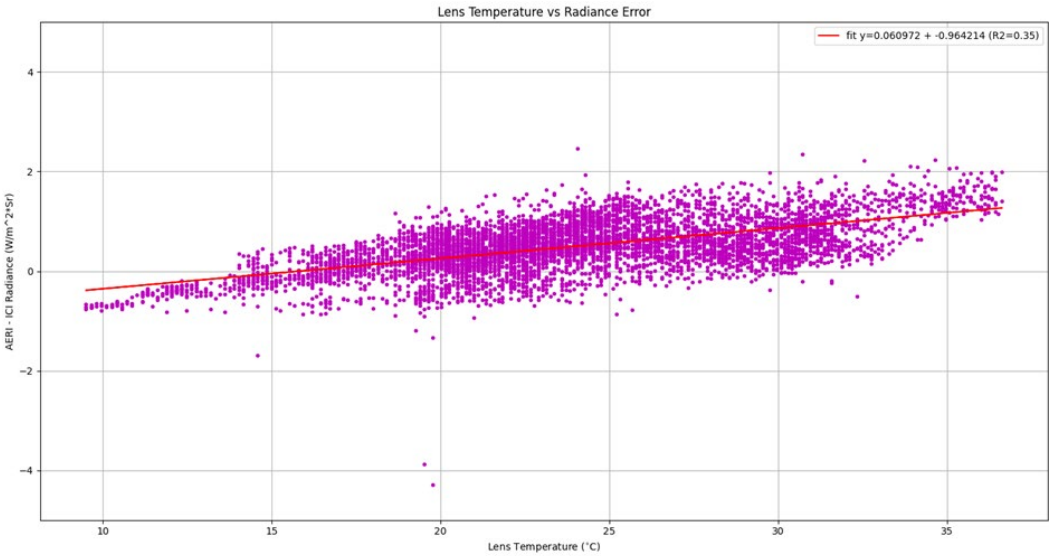

Figure 2. ICI-minus-AERI radiance versus lens temperature for original calibration method.

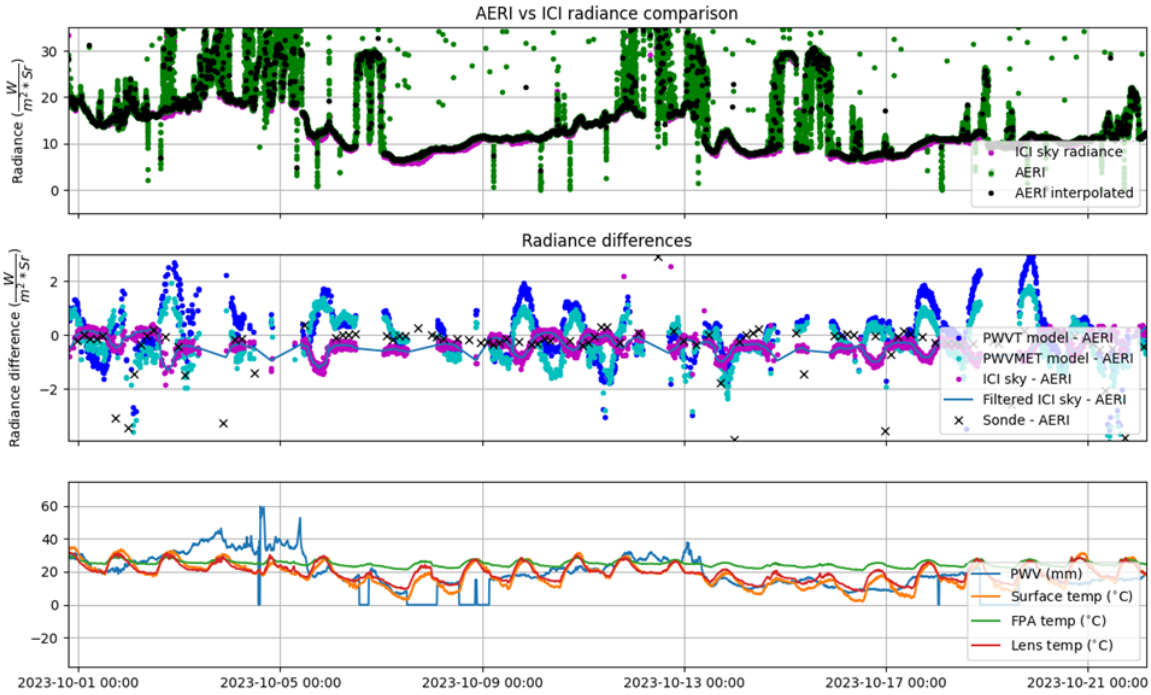

Figure 3. Example time series of ICI, AERI, and cloud-free model errors.

The upper axis of Figure 3 shows a time series of the ICI and AERI radiances. Clear-sky periods are typically smooth and slow moving, while cloudy periods exhibit quick changes in the zenith radiance.

The second axis of Figure 3 shows a time series of the ICI-minus-AERI radiance differences. Differences between the AERI and the radiances simulated by MODTRAN (Berk et al. 1999) using the data from SGP ARM balloon-borne sondes (Keeler et al. 2022) are shown for context. Some diurnal oscillations are apparent in the ICI-minus-AERI radiance. They typically have a peak-to-peak magnitude of 0.5 W/m^{2}Sr but can sometimes be as much as 1 W/m^{2}Sr. These are associated with the residual calibration error caused by the flat field correction in the camera and were previously known to be near the 0.5 W/m^{2}Sr level.

The accuracy of the calibration and models during clear-sky periods are the most interesting to us, because errors in the observed and modeled radiances limit the ability of the algorithms to detect thin clouds, which are important to our customers. To quantify the differences observed during clear-sky periods, we chose times when the AERI radiances were below 20 W/m^{2}Sr and stable within 0.5 W/m^{2}Sr from observation to observation. This constrained the analysis to periods that mostly consisted of clear skies. Figure 4 shows a histogram of ICI-minus-AERI differences during these times. A small bias exists between the instruments, but the dominant error appears to be the variation in the camera output due to the flat field correction (as mentioned above). The "sky radiance" shown are the calibrated radiance minus a fixed-pattern correction (FPC) that is derived after deployment. The FPC uses clear skies to characterize small but significant spatial non-uniformities resulting from our calibration setup. The "sky radiance" values were slightly farther from the AERI than the calibrated radiances (-0.39 versus -0.17). While this bias is small, it suggests that the FPC can introduce a small but significant bias. We also note that the ICI tends to undermeasure the radiance of very warm clouds by ~1 W/m^{2}Sr. Deviations of the camera response or laboratory calibration black body emissivity from those advertised by the vendors could cause these errors at higher radiances. Without further analysis, the exact source of this error was not immediately identifiable.

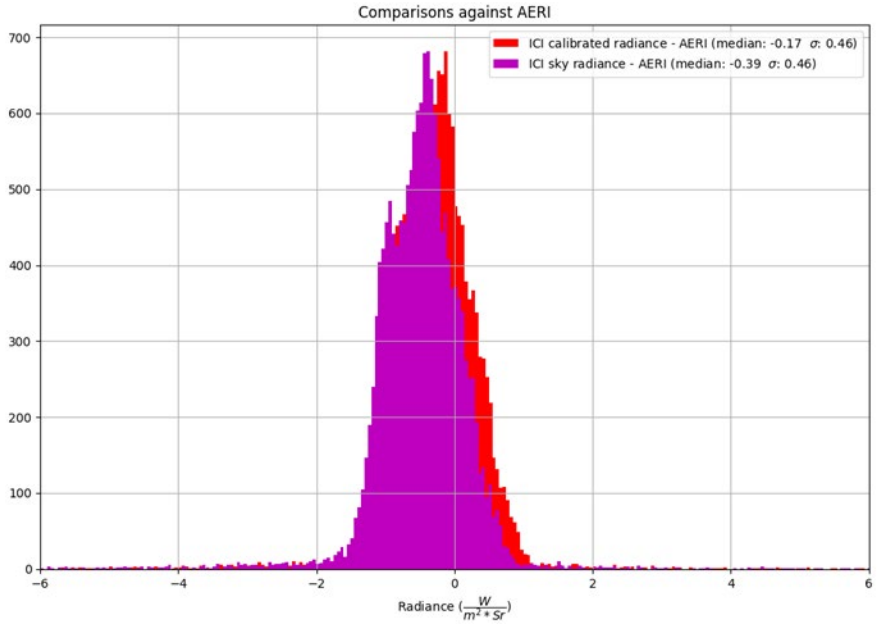

Figure 4. Histogram of differences between ICI and AERI radiances.

The second axis of Figure 3 shows a time series of two cloud-free models developed by NWB Sensors. The first uses PWV, surface temperature, surface barometric pressure, and carbon dioxide mixing ratio as

inputs. This model is designated the PWV+T. The second model uses these same inputs but also adds surface humidity. It is called the PWV+MET. This second model, the PWV+MET, is used operationally in the instrument. A time series of the difference between the radiances predicted by each of these models and those observed by the AERI is shown in the second axis of Figure 3. Some of the extreme residuals in this plot are due to clouds, but low-level oscillations in the residuals are apparent even during clear-sky periods. After investigation, we believe that these oscillations are characteristic of the underlying physical model. Since the atmospheric radiance is modeled as a multiple of the surface temperature to the 4th power, any error in the effective emissivity of the atmosphere will manifest as an oscillation with temperature. Therefore, these oscillations are expected.

Figure 5 shows a histogram of differences between the radiances predicted by these models and those observed by the AERI. In addition, differences between the MODTRAN models of the radiosondes and the AERI radiances are also shown for context. These error statistics are consistent with the residuals observed during model development. (These models were developed by simulating the downwelling radiance from over 7 million historical radiosondes.) The cloud-free models are accurate, but a model of the downwelling radiance based on surface parameters alone will have limited accuracy.

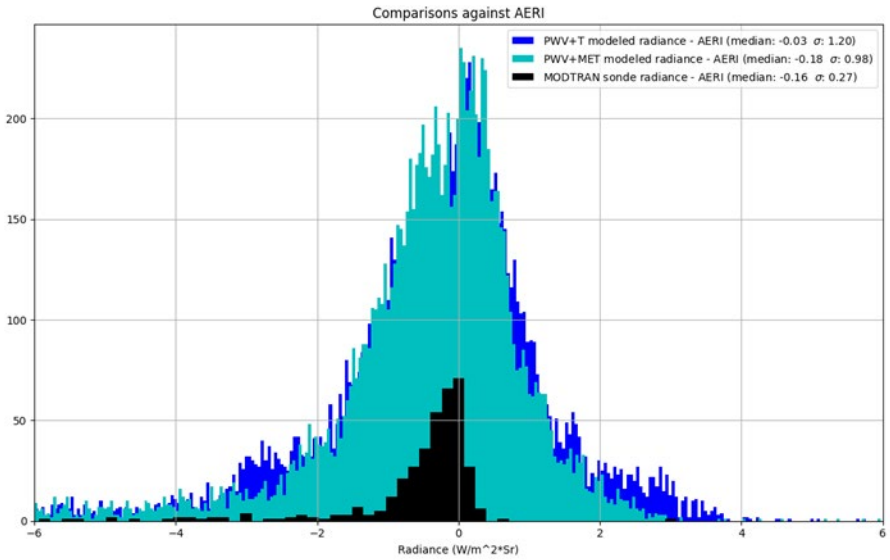

Figure 5. Differences between the NWB-developed cloud-free modeled radiances, MODTRAN-modeled radiances of sondes, and AERI radiances.

These results show that both the ICI camera calibration and the cloud-free models are very accurate, but modeling the cloud-free atmosphere using only surface data has limited precision. The ability of the ICI to confidently detect thin clouds is limited by the uncertainty in the models. Still, we are very satisfied with the ability of the instrument to create high-quality radiance and cloud data products.

3.0 Publications and References

Berk, A, GP Anderson, LS Bernstein, PK Acharya, H Dothe, MW Matthew, SM Adler-Golden, JH Chetwynd Jr., SC Richtsmeier, B Pukall, CL Allred, LS Jeong, and ML Hoke. 1999. "MODTRAN4 radiative transfer modeling for atmospheric correction." In AM Larar, ed. Optical spectroscopic techniques and instrumentation for atmospheric and space research III. *Proceedings of SPIE* 3756, https://doi.org/10.1117/12/366388

Bevis, M, S Businger, TA Herring, C Rocken, RA Anthes, and RH Ware. 1992. "GPS meteorology: Remote sensing of atmospheric water vapor using the global positioning system." *Journal of Geophysical Research – Atmospheres* 97(D14): 15787–15801, https://doi.org/10.1029/92JD01517

Cadeddu, M, and M Tuftedal. 1993. Microwave Radiometer (MWRLOS), 1993-07-21 to 2025-11-03, Southern Great Plains (SGP), Central Facility, Lamont, OK (C1). Atmospheric Radiation Measurement (ARM) User Facility, https://doi.org/10.5439/1999490

Gero, J, R Garcia, D Hackel, B Ermold, and K Gaustad. 1995. "Atmospheric Emitted Radiance Interferometer (AERICH1), 2004-02-10 to 2025-11-02, Southern Great Plains (SGP), Central Facility, Lamont, OK (C1)." Atmospheric Radiation Measurement (ARM) User Facility, https://doi.org/10.5439/1989299

Keeler, E, K Burk, and J Kyrouac. 2022. "Balloon-Borne Sounding System (SONDEWNPN), 2001-04-01 to 2025-11-02, Southern Great Plains (SGP), Central Facility, Lamont, OK (C1)." Atmospheric Radiation Measurement (ARM) User Facility, https://doi.org/10.5439/1595321

NWB Sensors. "Infrared Cloud Imager." https://www.nwbsensors.com/infrared-cloud-imager

www.arm.gov

U.S. DEPARTMENT OF
ENERGY

Office of Science